CHEMICAL ENGINEERING TRANSACTIONS
VOL. 70, 2018
A publication of AIDIC
The Italian Association of Chemical Engineering
Online at www.aidic.it/cet
Guest Editors: Timothy G. Walmsley, Petar S. Varbanov, Rongxin Su, Jiří J. Klemeš

ISBN 978-88-95608-67-9; **ISSN** 2283-9216
DOI: 10.3303/CET1870299

Industrial Heat Pump Integration in Non-Continuous Processes Using Thermal Energy Storages as Utility – An NLP Enhancement of the Graphical Approach

Jan A. Stampfli[a,b,*], Martin J. Atkins[b], Donald G. Olsen[a], Beat Wellig[a], Michael R. W. Walmsley[b], James R. Neale[b]

[a]Lucerne University of Applied Sciences and Arts, Competence Center Thermal Energy Systems and Process Engineering, Technikumstrasse 21, 6048 Horw, Switzerland
[b]University of Waikato, Energy Research Center, Private Bag 3105, 7 Hamilton 3240, New Zealand
jan.stampfli@hslu.ch

The aim of this paper is to enhance the results of the graphical approach for Heat Pump (HP) integration in non-continuous processes. A nonlinear programming (NLP) formulation is developed which optimizes temperature levels of condensation, evaporation, and storage temperature layers in order to further reduce total annual cost (TAC) and greenhouse gas (GHG) emissions. In addition, the NLP formulation requires low computation time given the practical approach. By its application on an AMMIX butter production of a large dairy factory, it is shown, that the temperature differences in the condenser and evaporator are reduced sharply which improves the COP of the HP from 2.2 to 3.4. As a result, the TAC can be reduced by an additional 16,721 NZD/y and the GHG emissions by an additional 29 t_{CO2}/y in comparison to the graphical approach.

1. Introduction

Within industrial sites the use of heat recovery (HR) is an effective method to reduce energy needs and improve efficiency. However, despite the continuous operation of the individual processes on the site, time dependency created by cleaning cycles, product change, shift work, etc. can result in a limitation of direct HR potential (Atkins et al., 2009). The result is effectively non-continuous process operation with changing process requirements. To overcome this challenge, the use of storage tanks as utility to allow the use of a Heat Pump (HP) to operate continuously despite the non-continuous process behavior is proposed.
In contrast to complex mathematical programming approaches as in Becker and Maréchal (2012), a practical methodology developed in a previous paper (Stampfli et al., 2018) uses graphical Pinch Analysis techniques such as the Grand Composite Curve (GCC) and the Time Pinch Analysis (Wang and Smith, 1995) for industrial HP integration in non-continuous processes. This approach allowed the determination of the overall HP condensation and evaporation temperature levels through the developed COP Curves. The temperature differences in both the condenser, evaporator and the specific heat exchangers (HEXs) used to transfer heat from or to the process streams are constrained by a fixed minimum temperature difference. It is shown, that this approach leads to a minimum HP size and maximized thermal energy storage (TES) capacities. Nevertheless, the assumed temperature differences in condenser and evaporator tend to be too large.
To help overcome the minimal temperature difference constraints and to find an economic optimum, in this paper a nonlinear programming (NLP) extension of the graphical approach which enhances the graphical results, is presented. Therefore, the total annual cost (TAC) is minimized using condensation, evaporation temperatures and the TES temperature levels as dependent optimization variables. To ensure, the practical applicability in terms of computation time and resources, the HP cycle is simplified as a Carnot cycle with a realistic Carnot efficiency.
The resulting model is applied to the same dairy case study as the graphical approach, whereby HR between an anhydrous milk fat (AMF) production plant, a cream treatment (CT) plant and their cleaning-in-place (CIP)

Please cite this article as: Stampfli J.A., Atkins M.J., Olsen D.G., Wellig B., Walmsley M.R.W., Neale J.R., 2018, Industrial heat pump integration in non-continuous processes using thermal energy storages as utility – an nlp enhancement of the graphical approach , Chemical Engineering Transactions, 70, 1789-1794 DOI:10.3303/CET1870299

system is analyzed and compared. The cost savings due to the integration of the HP-TES system are presented as well as the impact on greenhouse gas (GHG) emissions.

2. Methodology

This methodology extends the graphical approach for HP integration in non-continuous processes (Stampfli et al., 2018) with a NLP formulation which minimizes the TAC as a function of the HP, storage, HEX sizes, and the needed electricity demand of the HP. The superstructure of the model is shown in Figure 1. For a clear overview, optimization variables are represented in bold. The constant condensation $\boldsymbol{T_{co}}$ and evaporation $\boldsymbol{T_{ev}}$ temperatures of the HP as well as the storage temperatures $\boldsymbol{T_{H/C,h/c}}$ and the corresponding mass inventories of the storage layers $\boldsymbol{M_{H/C,h/c,l}}$, which are changing with time, are the optimization variables. As input variables, the matches between process streams (subscripts *i*: hot stream, *j*: cold stream, *l*: Time Slice (TS)) and HP-TES system, the corresponding heat flows $\dot{Q}_{i/j,l}$, and the supply and target temperatures $T_{i/j,l,S/T}$ of the process streams are given from the results of the graphical approach and used as input data for the optimization. The model is formulated and optimized using open source software from COIN-OR (computational infrastructure for operations research) (Lougee-Heimer, 2003). As algebraic modelling language, the python package pyomo (python optimization modelling objects) (Hart et al., 2017) and as NLP solver, Ipopt (interior point optimizer) (Wächter and Biegler, 2006) are used.

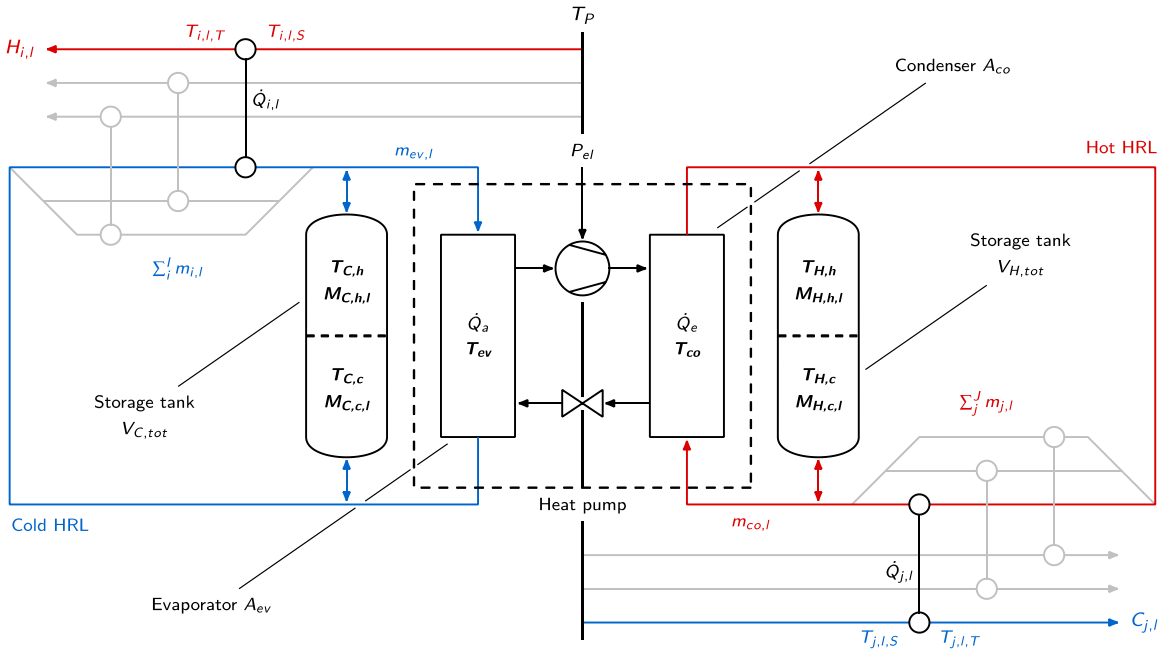

Figure 1: Superstructure of the HP-TES system

2.1 Temperature constraints

To ensure heat transfer between the process streams and the heat recovery loops (HRLs), the temperature levels of the layers (hot layer: *h*, cold layer: *c*) for the cold storage (*C*) have to be lower than the supply and target temperatures of the hot process streams which is given by

$$T_{i,l,S} \geq T_{C,h} \qquad T_{i,l,T} \geq T_{C,c} \qquad \forall i, \forall l \tag{1}$$

and the temperature levels of the hot storage (*H*) have to be higher than the supply and target temperatures of the cold process streams which is given by

$$T_{j,l,S} \leq T_{H,h} \qquad T_{j,l,T} \leq T_{H,c} \qquad \forall j, \forall l \tag{2}$$

Further, to ensure heat transfer between the HRLs and the HP, with

$$T_{ev} \leq T_{C,c} \leq T_{C,h} \tag{3}$$

the evaporation temperature T_{ev} has to be lower than the temperatures of the cold storage and the condensation temperature T_{co} has to be higher than the hot storage temperatures which is given by

$$T_{H,c} \leq T_{H,h} \leq T_{co} \tag{4}$$

2.2 Heat exchanger

The needed HEX area between process streams and the HP-TES system is given by

$$A_{i/j} = \max_l \left(\frac{\dot{Q}_{i/j,l}}{U_{i/j} \cdot \mathrm{LMTD}_{i/j,l}} \right) \qquad \forall i/j \tag{5}$$

where $U_{i/j}$ is the overall heat transfer coefficient between process stream and storage media and LMTD is the corresponding logarithmic mean temperature difference. Due to the fact, that there is no variation in time for the condenser and evaporator, their areas are given by

$$A_{co/ev} = \frac{\dot{Q}_{co/ev}}{U_{co/ev} \cdot \mathrm{LMTD}_{co/ev}} \tag{6}$$

For algorithmic robustness, the LMTD in each HEX is determined using the approximation from Chen (1987) which is given by

$$\mathrm{LMTD} \approx \left(\Delta T_1 \cdot \Delta T_2 \left(\frac{\Delta T_1 + \Delta T_2}{2} \right) \right)^{\frac{1}{3}} \tag{7}$$

This approximation underestimates the LMTD slightly which results in an overestimated area. The temperature differences for matches between hot process streams and the HP-TES system are given by

$$\Delta T_1 = T_{i,l,S} - T_{C,h} \qquad \Delta T_2 = T_{i,l,T} - T_{C,c} \qquad \forall i, \forall l \tag{8}$$

For the matches between cold process stream and the HP-TES system, the temperature differences are given by

$$\Delta T_1 = T_{H,h} - T_{j,l,T} \qquad \Delta T_2 = T_{H,c} - T_{j,l,S} \qquad \forall j, \forall l \tag{9}$$

The temperature differences in evaporator are given by

$$\Delta T_1 = T_{C,h} - T_{ev} \qquad \Delta T_2 = T_{C,c} - T_{ev} \tag{10}$$

and in the condenser given by

$$\Delta T_1 = T_{co} - T_{H,h} \qquad \Delta T_2 = T_{co} - T_{H,c} \tag{11}$$

Thereby, the superheating in the evaporator as well as the de-superheating and subcooling in the condenser are not considered for the LMTD.

2.3 Mass balance heat recovery loops

The needed volumes of the cold and hot storage are given by

$$V_{C/H,tot} = \frac{M_{C/H,h,l} + M_{C/H,c,l}}{\rho_{sm}} \qquad \text{for } l = 1 \tag{12}$$

where $M_{C/H,h/c}$ are the mass inventories of the hot and cold layer of the corresponding storage. ρ_{sm} represents the density of the storage media. Due to the mass balance, the sum of both mass inventories has to be constant over time. Therefore, the storage volume can be determined using the mass inventories of the first TS. To calculate the mass inventories of the temperature layers at the end of each TS, the mass balance is applied as follows

$$M_{C,h,l+1} = M_{H,h,l} + \sum_{i=1}^{I} (m_{i,l}) - m_{ev,l} \qquad \forall l \tag{13}$$

$$M_{C,c,l+1} = M_{C,c,l} - \sum_{i=1}^{I} (m_{i,l}) + m_{ev,l} \qquad \forall l \tag{14}$$

$$M_{H,h,l+1} = M_{H,h,l} - \sum_{j=1}^{J} (m_{j,l}) + m_{co,l} \qquad \forall l \tag{15}$$

$$M_{H,c,l+1} = M_{H,c,l} + \sum_{j=1}^{J}(m_{j,l}) - m_{co,l} \qquad \forall l \qquad (16)$$

Thereby, the mass inventories have to be bigger or equal to zero over time which is given by

$$M_{H/C,h/c,l} \geq 0 \qquad \forall l \qquad (17)$$

The transferred mass due to the heat flow from or to the process streams is given for each TS by

$$m_{i/j,l} = \frac{\dot{Q}_{i/j,l} \cdot \Delta t_l}{c_{p,sm} \cdot (T_{C/H,h} - T_{C/H,c})} \qquad \forall i/j, \forall l \qquad (18)$$

where $c_{p,sm}$ is the specific heat capacity of the storage media and Δt_l the TS duration. The transferred mass through evaporator and condenser are given by

$$m_{ev/co,l} = \frac{\Delta t_l}{\sum_{l=1}^{L} \Delta t_l} \cdot \sum_{i/j=1}^{I/J} \sum_{l=1}^{L} m_{i/j,l} = \dot{m}_{ev/co} \cdot \Delta t_l \qquad \forall l \qquad (18)$$

2.4 Heat pump cycle

The absorbed heat by the evaporator is defined by

$$\dot{Q}_a = \dot{m}_{ev} \cdot c_{p,sm} \cdot (T_{C,h} - T_{C,c}) \qquad \forall l \qquad (19)$$

and the emitted heat from the condenser by

$$\dot{Q}_e = \dot{m}_{co} \cdot c_{p,sm} \cdot (T_{H,h} - T_{H,c}) \qquad \forall l \qquad (20)$$

The HP cycle is simplified by the use of the definition of the COP

$$\mathrm{COP} = \zeta \cdot \frac{T_{co}}{T_{co} - T_{ev}} = \frac{\dot{Q}_e}{P_{el}} \qquad \forall l \qquad (21)$$

where ζ is a realistic Carnot efficiency. With the energy balance of the HP system as given by

$$\dot{Q}_e = \dot{Q}_a + P_{el} \cdot \eta_{drive} = \dot{Q}_a + P_i \qquad (22)$$

the electricity demand P_{el} and the corresponding input power into the refrigerant P_i for the HP system is determined.

2.5 Economics and emissions

The Objective function of the optimization represents the minimization of the TAC which is given by

$$\mathrm{TAC} = \frac{i\,(1+i)^n}{(1+i)^n - 1} \cdot \sum_E \left(F_E \cdot \frac{\mathrm{I_{PMEI2}}}{\mathrm{I_{PMEI1}}} \cdot \mathrm{MPIC}_E\right) + C_{op,a} \quad \text{with} \quad \mathrm{MPIC}_E = C_{E,0} + C_{E,1}\, Q^{f_{E,d,1}} + C_{E,2}\, Q^{f_{E,d,2}} \qquad (23)$$

Whereby i is the interest rate and n is the investment period. By the use of Lang factors F_E (Lang, 1948) installation, piping, control system, building, site preparation, and service facility cost of the corresponding equipment E are included. With the plant, machinery, equipment group index ($\mathrm{I_{PMEI}}$) of the capital goods price index (CGPI) (Stats NZ, 2017), the main plant item cost (MIPC) is corrected in terms of inflation and deflation. Corresponding equipment coefficients (C_E, $f_{E,d}$) for given capacities Q are listed in Stampfli et al. (2018). The operating cost is given by

$$C_{op,a} = P_{el} \cdot \sum_{l=1}^{L} (\Delta t_l) \cdot d \cdot c_{el} \qquad (24)$$

where c_{el} is the specific electricity cost. The number of days per year is given by d = 365. Further by

$$\mathrm{CO_2e} = P_{el} \cdot \sum_{l=1}^{L} (\Delta t_l) \cdot d \cdot \xi_{el} \qquad (25)$$

the annual GHG emissions are determined. Thereby, ξ_{el} is the specific CO_2e-emissions.

3. Dairy factory case study

The methodology is applied to an AMMIX butter production of a large dairy factory that includes, an AMF production plant, a CT plant, and their CIP system. The input data, which are the selected matches between

process streams and HP-TES system of the graphical approach is listed in Table 1. Further details to the process can be found in Stampfli et al. (2018).

Table 1: Matches between process streams and HP-TES system from the graphical approach.

Stream	TS_2 (8 -10 h)			TS_3 (10-15.5 h)			TS_4 (15.5-17.5 h)		
	T_S (°C)	T_T (°C)	$\dot{Q}$ (kW)	T_S (°C)	T_T (°C)	$\dot{Q}$ (kW)	T_S (°C)	T_T (°C)	$\dot{Q}$ (kW)
C_1: Cream heating (AMF)	-	-	-	15.4	31.7	236.7	15.4	31.7	236.7
H_1: Buttermilk cooling (AMF)	-	-	-	15.4	8	103.1	15.4	8	103.1
H_2: Trd. cream cooling (CT)	18.5	15.5	44.4	18.5	15.5	44.4	-	-	-
C_2: Pre rinse water (CIP)	20	27.6	7	20	26.6	6.1	20	27.6	7
C_3: Alkaline solution (CIP)	20	29.3	17	20	28.1	14.9	20	29.3	17
C_4: Nitric acid (CIP)	20	27.6	9.3	20	26.6	8.2	20	27.6	9.3
H_3: Post rinse water (CIP)	20	15	4.6	20	15	2.1	20	15	4.6

4. Results and discussion

In Table 2, the resulting temperature levels for the HP-TES system for the graphical method and the NLP enhancement are displayed. It can be seen, that the temperature lift is reduced by 18.95 K and thus the COP is improved from 2.2 to 3.4. Thereby, the temperature levels of the storage layers are only slightly adjusted. The temperature difference in the cold storage is increased by 0.19 K and in the hot storage reduced by 0.21 K. Due to this, the needed volume and the resulting cost is reduced for the cold storage yet increased for the hot storage, as shown in Table 3. The capacities of the needed equipment and the corresponding capital cost are displayed. Further, the HEX LMTDs are shown in brackets in the capacity column.

Table 2: Resulting temperature levels for the graphical method and the NLP enhancement.

Approach	T_{co} (°C)	T_{ev} (°C)	$T_{C,h}$ (°C)	$T_{C,c}$ (°C)	$T_{H,h}$ (°C)	$T_{H,c}$ (°C)
Graphical method	46.26	-4.56	8.00	2.94	38.76	30.00
NLP enhancement	36.23	4.36	10.06	4.81	35.64	27.09

Table 3: Comparison of HP-TES system using the graphical approach and the NLP enhancement. The resulting LMTDs are shown in brackets in the capacity column.

Equipment	Capacity unit	Capacity ([Q])				Capital cost (NZD)	
		Graphical method		NLP enhancement		Graphical method	NLP enhancement
Compressor	P_i (kW)	35		22.8		256,829	180,075
Motor	P_{el} (kW)	39		25.4		23,218	16,454
Evaporator	A (m^2)	3.4	(10.53 K)	16.7	(1.99 K)	6,589	15,385
Condenser	A (m^2)	5.3	(11.32 K)	20.3	(2.97 K)	7,877	17,794
Cold TES	V (m^3)	136		112.1		28,807	25,648
Hot TES	V (m^3)	133		136.0		28,359	28,777
Total HP-TES						351,679	284,133
HEX C_1	A (m^2)	57.0	(10.38 K)	83.2	(7.11 K)	42,091	59,387
HEX H_1	A (m^2)	41.9	(6.16 K)	61.8	(4.17 K)	32,062	45,220
HEX H_2	A (m^2)	9.7	(11.50 K)	11.7	(9.52 K)	10,738	12,064
HEX C_2	A (m^2)	0.6	(11.04 K)	0.9	(7.56 K)	4,768	4,962
HEX C_3	A (m^2)	1.6	(10.33 K)	2.5	(6.71 K)	5,438	6,025
HEX C_4	A (m^2)	0.8	(11.04 K)	1.2	(7.56 K)	4,906	5,163
HEX H_3	A (m^2)	0.4	(12.03 K)	0.5	(10.07 K)	4,602	4,651
Total HEX	A (m^2)	81.2		160.7		104,605	137,472
Total capital cost						456,284	421,605

The reduction of the temperature lift is attributable to the smaller LMTDs in the condenser and evaporator. As a result, the COP is increased and thus, the compressor power and its cost, which has the highest impact on the capital cost of the system, is reduced by around 70,000 NZD. Due to the high film heat transfer coefficients of the refrigerant caused by the phase transition in the condenser and evaporator (5,000 W/(m^2K)), the LMTD is reduced sharply with just a slight increase in HEX area. Generally, the LMTDs in the HEX are reduced and as a result, the area increased for the HEX between process streams and the HP-TES system. Nevertheless, in total, the capital cost for the HP-TES system and the HEXs is further reduced by 7.6 %. Due to the reduced electricity consumption, the annual operating cost can be further reduced by 16,721 NZD/y to 96,877 NZD/y. The TAC for the process design with included HP-TES system is reduced to 405,206 NZD/y which is now 16,963 NZD/y lower than the TAC for the process design without HP-TES system. The graphical method reduced the CO_2e-emissions by 117 t_{CO2}/y (27.0 % reduction) and by applying the NLP enhancement method presented here further reduced the CO_2e-emissions by an additional 29 t_{CO2}/y (6.6 % reduction) to an overall total CO_2e-emissions of 294 t_{CO2}/y.
The computation duration was about 0.5 s on a notebook with an i7 Dual Core processor and 16 GB RAM. Therefore, the model is not expensive in forms of computation time and resources.

5. Conclusions

With the NLP enhancement, the results of the graphical approach are further improved by the reduction of TAC and GHG emissions. Thereby, the temperature differences in the HEX are reduced by tendency. In particular, the temperature differences in condenser and evaporator are reduced due to the high film heat transfer coefficients during the phase transition of the refrigerant. This leads to an improvement of the COP which causes a reduction in TAC and GHG emissions. The temperature differences in the storage tanks remain small after the optimization. This leads to large storage tanks, which could probably be improved by the use of latent storages instead of sensible stratified storages. In order to provide an exact statement, the resulting cost for latent storage including the phase change material require further analysis.
The developed NLP formulation is able to enhance the results of the graphical method and can be applied in practice with short computing time and low resource requirements. However, the matches between process stream and HP-TES system are based on relaxed pinch rules. To verify the selection of the matches, a mixed integer optimization should be formulated. Thereby, the temperature levels of the condenser and evaporator are no longer limited by the selected matches and thus, the solution space is less constrained.

Acknowledgments

This research project is financially supported by the Swiss Innovation Agency Innosuisse and is part of the Swiss Competence Center for Energy Research SCCER EIP.

References

Atkins M.J., Walmsley M.R.W., Neale J.R., 2009, The challenge of integrating non-continuous processes – milk powder plant case study, Chemical Engineering Transactions, 18, 445-450.
Becker H.C., Maréchal F., 2012, Targeting industrial heat pump integration in multi-period problems, Computer Aided Chemical Engineering, 31, 415-419.
Chen J.J.J., 1987, Comments on Improvements on a replacement for the logarithmic mean, Chemical Engineering Science, 42(10), 2488-2489.
Hart W.E., Laird C.D., Watson J.-P., Woodruff D.L., Hackebeil G.A., Nicholson B.L., Siirola J.D., 2017, Pyomo – optimization modelling in python. Second Edition, Vol. 67, Springer.
Lang H.J., 1948, Simplified approach to preliminary cost estimates, Chemical Engineering, 55(6), 112-113
Lougee-Heimer R., 2003, The common optimization interface for optimizations research: Promoting open-source software in the operations research community, IBM Journal of Research and Development, 47(1), 57-66.
Stampfli J.A., Atkins M.J., Olsen D.G., Wellig B., Walmsley M.R.W., Neale J.R., 2018, Industrial heat pump integration in non-continuous processes using thermal energy storages as utility – a graphical approach, Chemical Engineering Transactions, 70, 901-906.
Stats NZ, 2017, Price index by item – plant, machinery and equipment <www.stats.govt.nz/infoshare/> accessed 20.11.2017.
Wächter A., Biegler L.T., 2006, On the implementation of an interior-point filter line-search algorithm for large-scale nonlinear programming, Mathematical Programming, 106(1), 25-57.
Wang Y.P., Smith R., 1995, Time Pinch Analysis, Chemical Engineering Research & Design, 73(8), 905-914.